



BACCHUS

Impact of Biogenic versus Anthropogenic emissions on Clouds and Climate: towards a Holistic UnderStanding

Collaborative Project

SEVENTH FRAMEWORK PROGRAMME
ENV.2013.6.1-2

Atmospheric processes, eco-systems and climate change

Grant agreement no: 603445

Deliverable number:	D2.3
Deliverable name:	Parametrisations of the biogenic and anthropogenic organic compounds impact in new particle formation and growth to CCN and evaluation of associated uncertainties
WP number:	2
Delivery date:	Project month 36 (30/11/2016)
Actual date of submission:	01/12/2016
Dissemination level:	PU
Lead beneficiary:	UHEL
Responsible scientist/administrator:	Veli-Matti Kerminen
Estimated effort (PM):	33 PM
Contributor(s):	Veli-Matti Kerminen, Risto Makkonen, Stephany Mazon (UHEL); Ken Carslaw, Hamish Gordon (ULEEDS); Colin O'Dowd, Jurgita Ovadnevaite (NUIG); Matteo Rinaldi (CNR-ISAC), Urs Baltensperger, Josef Dommen, Chris Hoyle (PSI)

Estimated effort contributor(s) (PM):	UHEL: 16 PM, ULEEDS: 1 PM, NUIG: 10 PM, CNR-ISAC: 1 PM, PSI: 5 PM
Internal reviewer:	Maria Kanakidou

Objectives and executive summary

This deliverable aimed at the development of parametrisations for the impact of biogenic and anthropogenic organic compounds on new particle formation (NPF) and growth to CCN and evaluation of associated uncertainties. For this purpose, the latest CERN cloud and other chamber data and ambient CCN/aerosol datasets have been compiled and analysed to provide appropriate parameterisations for NPF and growth (section 1). The effects of NPF and growth in marine and coastal environments have been also studied using the high-resolution aerosol mass spectrometer measurement together with aerosol microphysics and CCN measurements during open ocean particle production events observed in Mace Head, Ireland. The CCN production from nucleation and organic vapour growth using the datasets constructed in Task 1.6 has been investigated. The approach of Kerminen et al. (2012) has been extended to analyse the CCN production associated with new particle formation and the role of organic vapors for particle growth from nucleation size to CCN sizes. The latest parameterisations of new particle formation and growth from the chamber studies have been used to evaluate the global implications using the global models of BACCHUS. Simulations separated the effect of natural and anthropogenic organic precursor gases on the CCN budget (section 2).

Global model simulations suggest that i) nucleation of sulphuric acid with oxidation products of α -pinene makes a major contribution to global particle concentrations and helps to explain the seasonal cycle of particle number concentration from biogenic emissions, and that ii) pure biogenic nucleation of the oxidation products of α -pinene enhances pre-industrial CCN concentrations by 20–100% across large areas of the northern hemisphere, thereby reducing considerably the anthropogenic aerosol-cloud radiative forcing. Simulations demonstrate that the treatment of early growth of nucleated particles by condensation of oxidised organic molecules substantially alters global CCN concentrations – by up to $\pm 50\%$ in comparison with previously assumed growth rate parameterizations. Global model simulations indicate that the CCN-effects of SOA formation are somewhat modulated by the representation of primary-emissions, and suggest that higher level of details in both timing and size-distribution of primary emissions would influence the SOA climate effects. Simulations with ELVOC-formation parameterizations indicate higher future CCN concentrations in Eastern Siberia due to increasing BVOC emissions.

Summary of results

1. Parameterizations of new particle formation and growth to CCN based on laboratory experiments and field measurements

1.1. Organic aerosol precursors and their oxidation in the atmosphere

Monoterpenes (MT) are thought to be globally the most important source of gaseous compounds responsible for the growth of newly-formed particles to CCN. There is, however, a serious lack of long-term continuous measurements of monoterpene concentrations in the ambient atmosphere. Motivated by this, we developed 5 slightly different proxies for the concentration of MT's based on continuous proton transfer reaction mass spectrometer (PTR-MS) measurements made at a boreal forest site in Hyytiälä, southern Finland, during the time period 2006–2013 (Kontkanen et al., 2016).

The proxies for the MT concentration take into account the temperature-controlled emissions from the forest ecosystem, dilution caused by the mixing within the boundary layer, and different oxidation processes. The most comprehensive of these proxies is given by:

$$[MT]_{proxy,ideal} = \frac{a \exp(b(T-T_s))}{k_{OH+MT}[OH] + k_{O_3+MT}[O_3] + k_{NO_3+MT}[NO_3]} \times BLH^c \times ws^d. \quad (1)$$

Here BLH is the boundary-layer height, ws is wind speed, k_{OH+MT} , k_{O_3+MT} and k_{NO_3+MT} are reaction rates between MT and different oxidants, and a , b , c and d are coefficients obtained by fitting Eq. 1 to the measurement data. The 4 other MT concentration proxies are simplifications of Eq. 1. Figure 1 shows the correlation between the proxy given by Eq. 1 and measured MT concentrations, while Figure 2 illustrate the performance of all the 5 MT proxies over different time scales. All the proxies captured the seasonal variation of the MT concentration, In addition to which they described the diurnal variation of the monoterpene concentration rather well, especially in summer months.

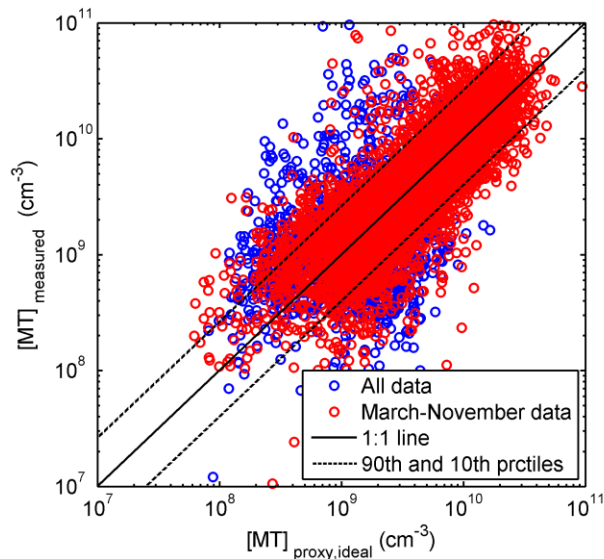


Figure 1. The correlation between the measured MT concentration and concentration predicted by Eq. 1 (Kontkanen et al., 2016).

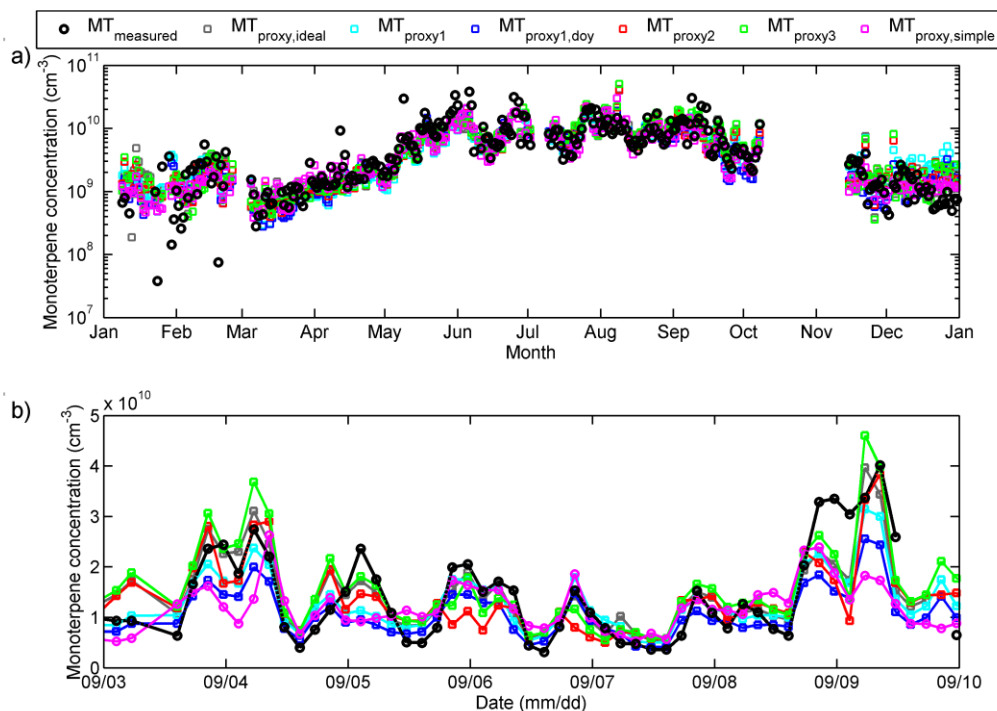


Figure 2. Time series of the measured MT concentration and the concentrations predicted by different proxies (a) for the whole year 2013, (b) for one week in September 2013 (Kontkanen et al., 2016). In case of one of the proxies, two different formations of it (proxy1 and proxy1, doy) are shown.

Measurements of MT oxidation product concentrations are very scarce in the ambient atmosphere and, until present, no parameterization for this quantity exists. By utilizing the proxies for monoterpene concentration derived from observations as above described, the following proxy for the concentration of oxidation products of MT was developed:

$$[OxOrg] = \frac{(k_{OH+MT}[OH] + k_{O_3+MT}[O_3] + k_{NO_3+MT}[NO_3]) \times MT_{proxy}}{CS} \quad (2)$$

where CS is the condensational sink of organic vapors on preexisting aerosols. It should be noted that OxOrg can be thought to represent the total concentration of oxidized monoterpenes, because it takes into account all the generations of oxidation products, from the first oxidation until condensable molecules. However, as the formulation of this proxy presumes that oxidation takes place relatively fast and that there are no other sinks than condensation sink (CS), it should be considered as a rough estimate for the concentration of condensable organic vapors.

Most of the current modeling frameworks require the yields of organic compounds of different volatility to simulate aerosol formation and growth. The simplest classification in this regard is to divide all gaseous organic compounds into the following volatility classes (Donahue et al., 2011: extremely low-volatile (ELVOC), low-volatile (LVOC), semi-volatile (SVOC), intermediate-volatile (IVOC) and volatile (VOC) organic compounds. We conducted extensive laboratory experiments in an atmospheric pressure flow tube (TROPOS-LFT) in order to determine the ELVOC yields from five differently structured biogenic volatile organic compounds: two endocyclic (limonene and α -pinene) and one exocyclic (β -pinene) and one acyclic (myrcene) monoterpene as well as isoprene (Jokinen et al., 2015, Table 1 below).

Table 1. Total molar yields of ELVOC from selected terpene oxidation with uncertainty of –50/+100% arising from calibration

Yield	Limonene	α -Pinene	Myrcene	β -Pinene	Isoprene
Y (O ₃), %	5.3 (1.56)	3.4 (1)	0.47 (0.14)	0.12 (0.035)	0.01 (0.003)
Y (OH), %	0.93 (0.27)	0.44 (0.13)	1.0 (0.29)	0.58 (0.17)	0.03 (0.009)

The data in brackets represent ELVOC yields relative to the ozonolysis of α -pinene.

We observed that ELVOCs from all precursors are formed within the first minute after the initial attack of an oxidant. We found that under atmospherically relevant concentrations, species with an endocyclic double bond efficiently produce ELVOC from ozonolysis, whereas the yields from OH radical-initiated reactions are smaller. If the double bond is exocyclic or the compound itself is acyclic, ozonolysis produces less ELVOC and the role of the OH radical-initiated ELVOC formation is increased. Isoprene oxidation produces marginal quantities of ELVOC regardless of the oxidant.

Studies on ELVOC formation from anthropogenic precursors have also been conducted (Garmash et al, in preparation), focusing mainly on OH-initiated oxidation of aromatic compounds. This work is in many ways more challenging than with biogenic precursors, since the importance of multi-generation oxidation in ELVOC-formation is larger, due to the slow reaction rate of the initial aromatic precursors. Our preliminary findings suggest a very low (<1%) ELVOC yield from first generation benzene oxidation, but after further OH oxidation the molar yields of highly oxidized products (O/C>1) rise as high as 10% or more. Parametrizations of this process therefore requires further work, and investigations are under way.

1.2. New particle formation

1.2.1 NPF involving organic compounds

The initials steps of new particle formation (NPF) were investigated using CERN cloud chamber experiments. For a system having both gaseous sulfuric acid (H₂SO₄) and biogenic oxidized organic vapors (BioOxOrg), the formation rate of new particles, J , could be approximated with the following formulae (Riccobono et al., 2014):

$$J = k \times [\text{H}_2\text{SO}_4]^p \times [\text{BioOxOrg}]^q . \quad (3)$$

Here k is a multicomponent prefactor, and p (2.17±0.14) and q (0.80±0.23) are fits to the measured chamber data. Equation 3 confirms the important role of sulfuric acid in driving atmospheric NPF that was found in numerous field measurements (e.g. Kulmala et al., 2014), and suggests further that organic compounds participate in NPF at the very early stages. It should be noted that parameterizations similar to Eq. 3 have been derived based on field measurements of atmospheric NPF at several sites with different mixtures of oxidized organic compounds (Paasonen et al., 2010). Equation 3, while using somewhat different values of k , p and q , agrees broadly with these earlier parameterizations.

Concentrations of gaseous sulfuric acid are typically low at remote continental sites, or in the pre-industrial atmosphere exposed mainly to natural sulfur emissions. Kirkby et al. (2016) showed that at very low

gaseous sulfuric acid concentrations, new particle formation rate is affected by both ions and oxidized organic compounds: when the HOM concentration is low, ions significantly influence NPF, whereas at high HOM concentrations the formation of new particles is dominated by neutral pathways (Figure 3).

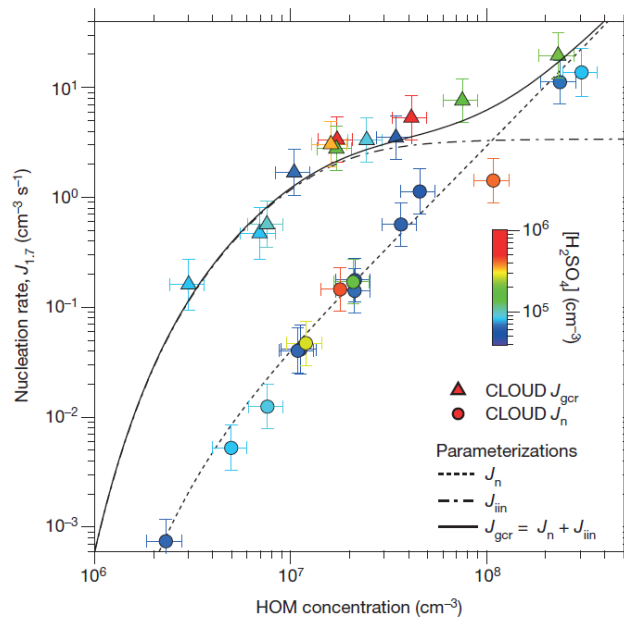


Figure 3. Formation rate of 1.7 nm particles as a function of gaseous HOM concentration, where HOM refers to highly-oxidized organic molecules. J_n is the new particle formation rate in the absence of ions, J_{iin} is the new particle formation rate initiated by ions, while J_{gcr} is the new particle formation rate when ion production is roughly equal to that observed close to the Earth surface because of the galactic cosmic rays (Figure taken from Kirkby et al., 2016).

Taken together, the CERN cloud chamber experiments suggest that NPF in the lower atmosphere may involve a mixture of two distinct mechanisms. The first, which is more important in polluted environments, involves clustering by sulfuric acid and water together with a combination of amines or ammonia with oxidized organics, and has a strong dependence on sulfuric acid. The second, which is more important in pristine environments, involves the formation of pure organic particles and depends on only oxidized organics and ions.

1.2.2. Marine new particle formation

Marine aerosol significantly contributes to the global radiation balance through the formation of haze and cloud layers reflecting incoming solar radiation (O'Dowd et al., 2010; Viashya et al., 2013). Secondary particles, resulting from gas-to-particle conversion, followed by condensation growth, or growth *via* heterogeneous chemical reactions, can potentially act as cloud condensation nuclei. Typically, secondary marine aerosol dominates the number concentration of the population and resides in the submicron size regime. It is considered that the predominant source of secondary marine aerosol is biogenic and related mainly to marine productivity (blooming plankton) which is responsible for the production of precursor gases such as Sulphur species (Charlson et al., 1987), nitrogen species (e.g. amines; Facchini et al., 2008) and organic matter (Dall'Osto et al., 2012).

A 9-year record of north east Atlantic aerosol size distributions (20 nm to 500 nm in diameter) at Mace Head was analysed for evidence of the occurrence of open ocean new particle formation and growth events. Evidence of new particle formation is regarded to the observation of a mature nucleation mode or a nascent ultrafine mode at sizes of 10–20 nm. Analysis of the 9-year record revealed that the average percentage occurrence of these events displayed a seasonal cycle with a peak of 35% occurring in May, and a minimum of 3% in January (Figure 4). Cluster analysis of 70 000 1-hour size distributions revealed four categories of size distributions: Anthropogenic/Continental European outflow, Clean Marine, Marine-Coastal Nucleation and Marine Open-Ocean Nucleation and Growth. The cluster analysis identified two modes in the open ocean particle production and growth cluster, one with a modal diameter of 18 nm and another with a modal diameter of 80 nm. The occurrence of the open ocean cluster was found to be highly correlated with oceanic chlorophyll-*a* with a correlation coefficient $r=0.83$ (Figure 5). These results link the formation of new particles in the marine boundary layer to the biological processes at the ocean surface using chlorophyll-*a* as a productivity proxy.

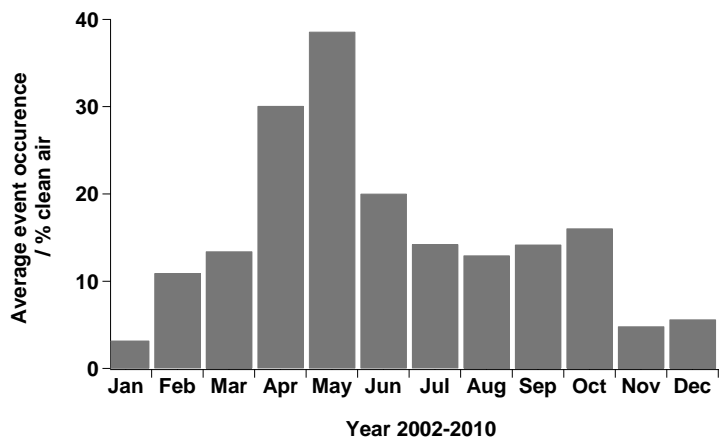


Figure 4. Seasonality of monthly frequency of occurrence of open ocean particle production and growth events in clean air masses at Mace Head from 2002 to 2010.

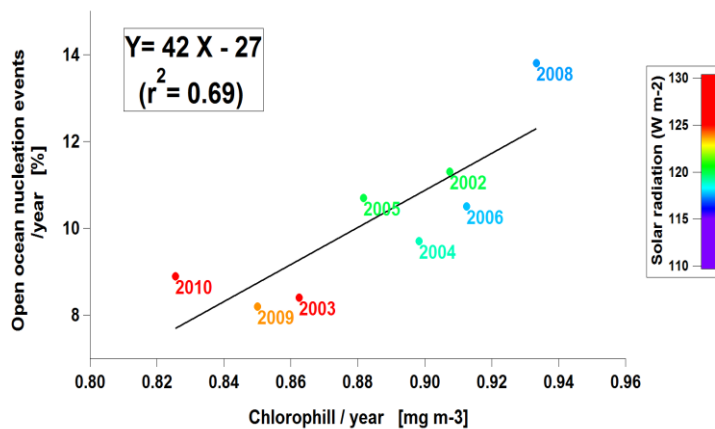


Figure 5. Monthly average frequency of occurrence of open ocean particle production events as a function of chlorophyll-*a* concentrations taken from the MODIS satellite measurements, for 24-

month-long averages over the years 2009 and 2010 and annual average values of the same parameters from the years 2002 to 2010.

A totally different NPF mechanism was identified in an iodine-rich, coastal environment (Fig. 6, Sipilä et al., 2016). We found that the formation and initial growth processes are driven almost exclusively by iodine oxoacids and iodine oxide vapors. The high molar oxygen-to iodine ratio (average 2.4) in the clusters together with the high observed concentrations of iodic acid (HIO_3) suggest that cluster formation primarily proceeds by sequential addition of HIO_3 , followed by intra-cluster restructuring to I_2O_5 and recycling of water either in the atmosphere or on dehydration. While the data presented in Figure 6 are from Mace Head, Ireland, observational support for this finding was also obtained from Northern Greenland and Queen Maud Land, Antarctica (Sipilä et al., 2016).

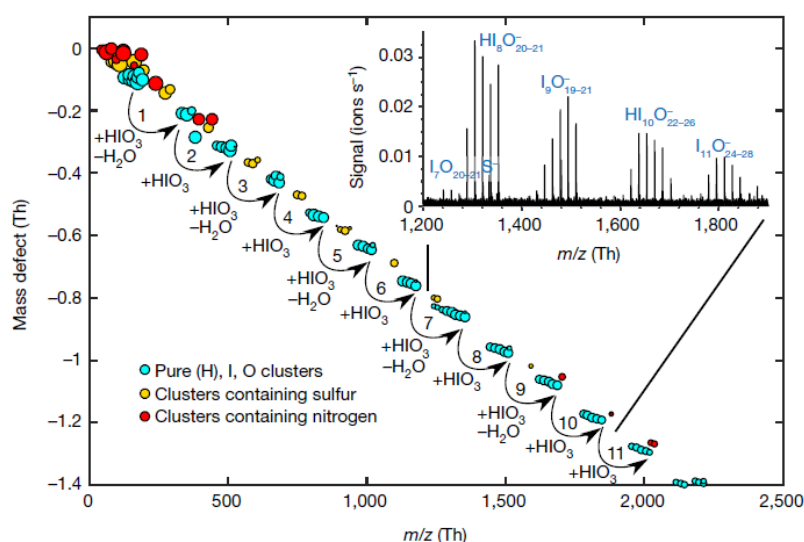


Figure 6. Plot of mass defect versus cluster mass depicting the abundance and atomic composition of neutral clusters participating in the observed NPF event. The area of the dots is proportional to the observed signal. The inset shows a portion of the recorded raw mass spectrum (Sipilä et al., 2016).

1.3. Growth of newly-formed particle to CCN

1.3.1 Chemistry and dynamics of particle growth

The CERN cloud chamber experiments have brought plenty of new insight into the growth of newly-formed aerosol particles. Lehtipalo et al. (2016) showed that ions can enhance the growth of sub-3 nm clusters containing sulfuric acid, but only if the growing clusters have not been stabilized by bases or organic compounds. Tröstl et al. (2016) quantified the role of organic compounds of different volatility on particle growth. They found that while ELVOC are the most important contributors to the particle growth at the smallest particle sizes, more volatile compounds tend to take over soon after the growing particle reach 2 nm in diameter (Fig. 7).

The results obtained from CERN cloud experiments agree with the schematic figure by Ehn et al. (2014) representing the growth of newly-formed particles to CCN (Fig. 8).

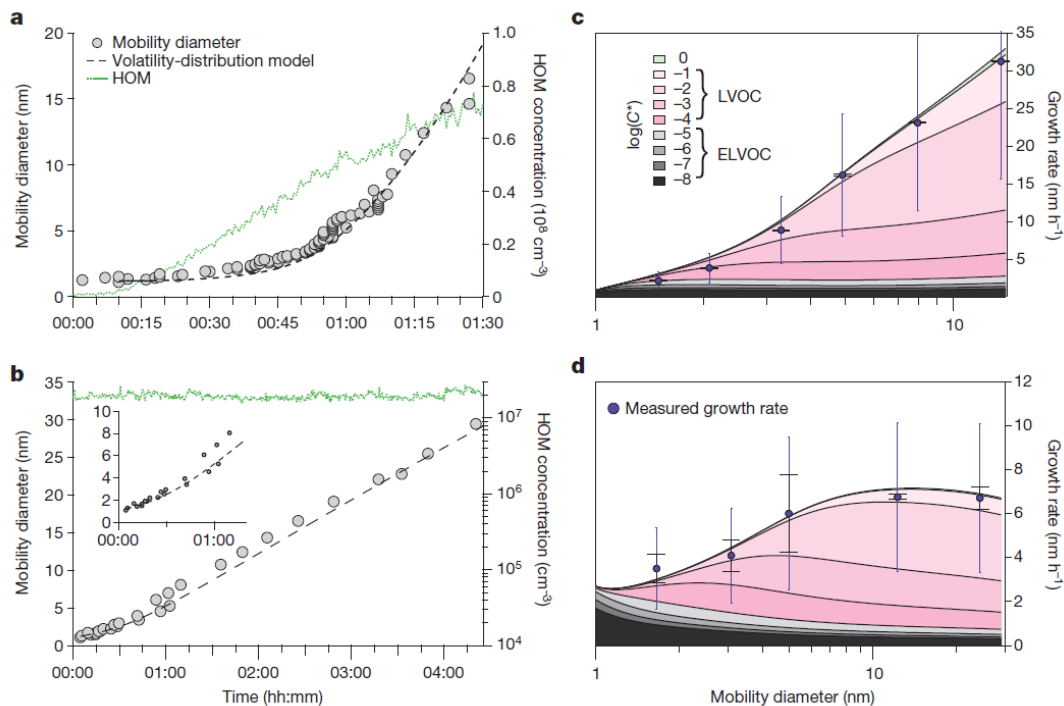


Figure 7. Comparison of the growth rates in two chamber experiments with a dynamic volatility basis set (VBS) model (Tröstl et al., 2016).

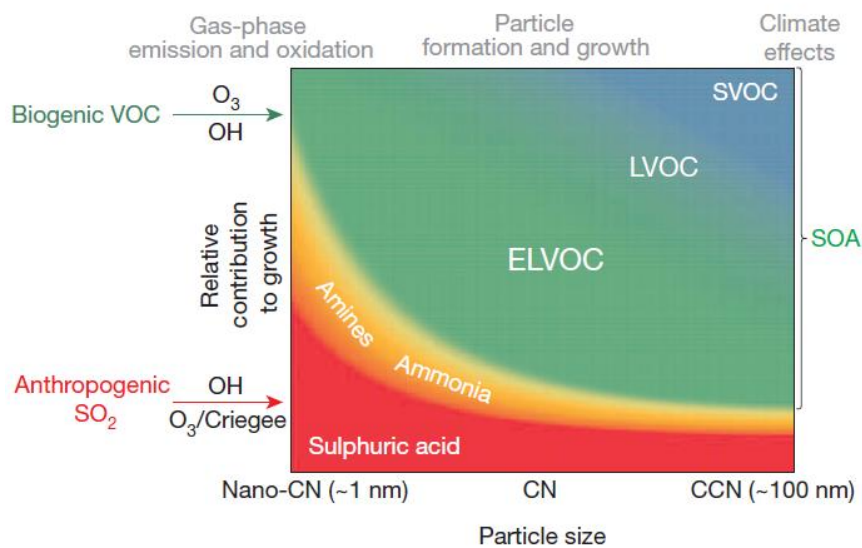


Figure 8. Schematic overview on the importance of precursor vapors for aerosol growth at different sizes (Ehn et al., 2014). The relative roles of different vapors will vary depending on location and prevailing meteorological conditions.

1.3.2. Parametrizing particle growth to CCN based on field measurements

We compiled 35 data sets of particle number size distribution measurements having each at 1 year of continuous measurement data (Fig. 9), and determined the following quantities from these data: the frequency of new particle formation event, formation rate of 10 nm diameter particles during such events and average growth rate of 10-25 nm particles during these events.

We found no clear environmental pattern for the NPF frequency, except that some rural sites showed high frequencies compared with other types of sites. Averaged over all the sites, the NPF frequency was the lowest during the winter (~10%) and highest during the spring (~30%). The production rates of 10 nm particles were the highest at urban sites and lower at less polluted sites. Averaged over all the sites, the formation rate of 10 nm particles was slightly below $1 \text{ cm}^{-3} \text{ s}^{-1}$ with a modest seasonal variation. The average growth rates of 10–25 nm particles varied from about 3 nm/hour (winter) to 4-5 nm/hour (summer), with no clear environment pattern but hints of biogenic and/or photochemical influence. Given the observed NPF event frequencies and durations, the formation rates of 10 nm particles and particle growth rates, one may conclude that 1) NPF probably dominates the particle number budget in remote and most rural locations, and possibly also in urban environments, and 2) NPF has clearly the potential to contribute significantly to the cloud condensation nuclei (CCN) budget over continental areas. A manuscript summarizing the results is in preparation.

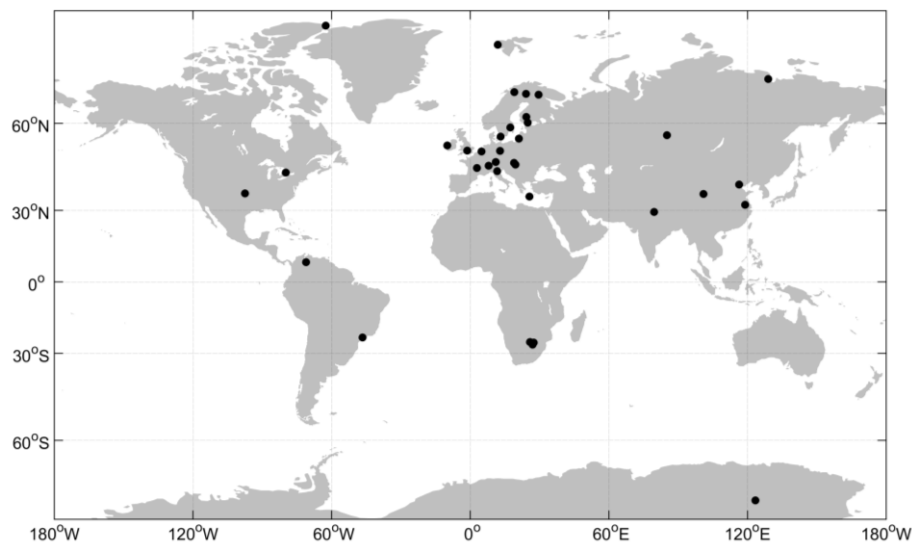


Figure 9. Locations of field sites, for which the characteristics of NPF was determined. The sites are categorized into the following sub-classes: polar, high-latitude, coastal/marine, remote continental, rural and urban sites.

We developed an automatic method, by which one can simultaneously determine the growth rate of nucleation, Aitken and accumulation mode particles using continuous particle number distribution measurements. So far, this tool has been applied to 16 long-term data sets. The analyzed data cover environments with very different anthropogenic influence: in the cleanest sites the particle growth is expected to be almost solely due to biogenic precursors, while in the most polluted sites the growth may be dominated by anthropogenic compounds. This analyses is currently extended to additional sites.

1.3.3. Analyzing CCN formation from NPF based on field measurements

Kerminen et al. (2012) discussed comprehensively how regional CCN formation associated with atmospheric new particle formation can be estimated from field observations, and what are the uncertainties related to such analyses. We have applied the approach introduced by Kerminen et al. (2012) to several long-term data sets.

As an example of our analyses, we obtained for the first time direct evidence on CCN production associated with atmospheric NPF in the Eastern Mediterranean atmosphere (Kalivitis et al., 2015). We found that both gaseous sulfuric acid and organic compounds play important roles in growing nucleated particles to CCN sizes in this environment during summertime. This case study demonstrated the power of simultaneous particle number size distribution, CCN and aerosols chemical measurements in investigating the origin of CCN in a polluted marine environment, as well as their limitations in distinguishing sources and sinks.

Another example is from a Yangtze River Delta region in China. In this highly-polluted continental environment, NPF formation occurs frequently during all the seasons except winter, and the observed new particle formation and growth rates are very high (Qi et al., 2015). The season-averaged diurnal behavior of the particle number size distribution reveals that NPF is strong source of CCN in this environment (Figure 10).

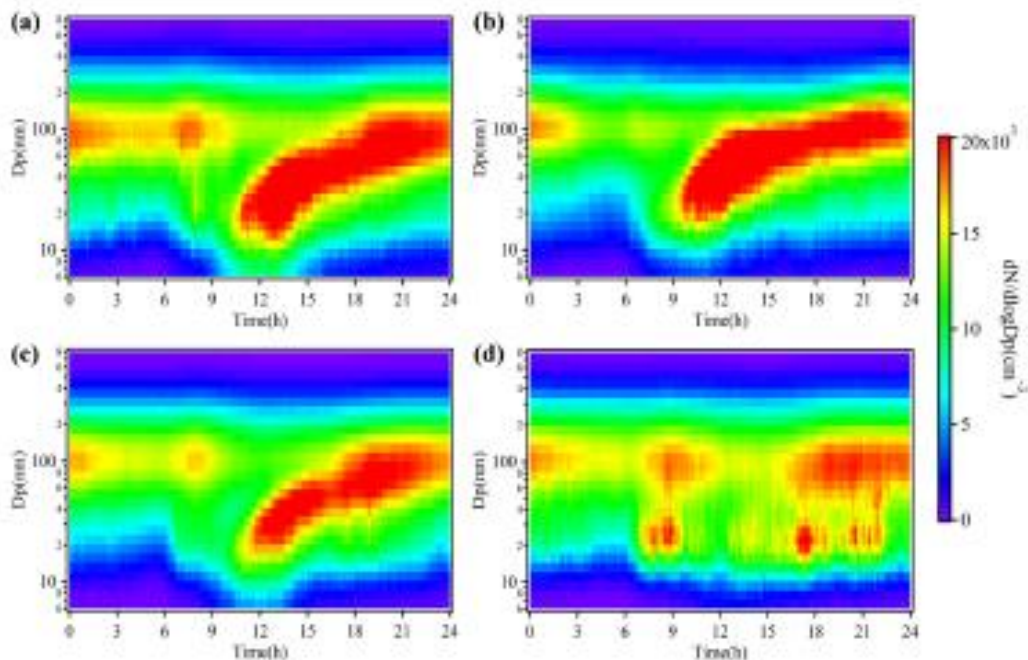


Figure 10. Averaged diurnal cycles of particle number size distributions for (a) spring, (b) summer, (c) autumn and (d) winter at the SORPES station in China during the 2-year measurement period (Qi et al., 2015).

2. Implementation into large-scale model frameworks

2.1 GLOMAP model

2.1.1. Model development

ULEEDS has implemented parameterisations of CERN CLOUD chamber nucleation measurements into the GLOMAP global aerosol model and explored the implications for global aerosol and radiative forcing. This is the first time that we can estimate the biogenic organic effects on global CCN based on what we consider to be the most complete model of global aerosol formation yet available. The focus has been on understanding aerosol formation in the natural pre-industrial (PI) atmosphere, although we are also able to update previous assessments of the present-day atmosphere.

Previous models of pre-industrial particle formation generally only accounted for the contribution of sulphuric acid to new particle formation (Merikanto et al., 2010; Kazil et al., 2010; Pierce and Adams, 2009). The Pierce and Adams study found that binary sulphuric acid nucleation rates were a factor 10 lower in the pre-industrial atmosphere, ternary rates involving ammonia a factor 5 lower, and boundary layer CCN concentrations increase by a factor of around 3.2 over the industrial period. The inclusion of organic nucleation reduces all these estimated changes.

New experimental data from the CERN CLOUD chamber (described above) now allow the contribution of ammonia and organic molecules to be assessed throughout the troposphere (Dunne et al., 2016). Experiments also show that highly oxidised organic molecules of biogenic origin can nucleate without sulphuric acid (Kirkby et al., 2016) and that this mechanism has a large effect on PI aerosols (Gordon et al., 2016).

The GLOMAP model was updated to include nucleation of mixtures of sulphuric acid, ammonia and highly oxidised organic molecules (HOMs) in the present-day and pre-industrial atmospheres. Nucleation rates at 1.7 nm mobility diameter are calculated as the sum of the following new parameterisations of CLOUD chamber data:

1. Binary nucleation of sulphuric acid (Dunne et al., 2016)
2. Ternary nucleation of sulphuric acid and ammonia (Dunne et al., 2016)
3. Nucleation of organics with sulphuric acid (Riccobono et al., 2014):

$$J_R = 0.5k_R[H_2SO_4]^2[BioOxOrg] \quad (4)$$

where BioOxOrg refers to the oxidation products of monoterpenes with OH, $k_R = 3.27 \times 10^{21}$, and the factor 0.5 corrects for the large yield of HOMs from α -pinene compared to other terpenes found in Jokinen et al. (2015).

4. Nucleation of organics alone, a sum of neutral (J_n) and ion-induced (J_{iin}) components from Gordon et al. (2016):

$$J_{org} = J_n + J_{gcr} \quad (5)$$

$$J_n = a_1[\text{HOM}]^{(a_2+a_5)/[\text{HOM}]} \quad (6)$$

$$J_{\text{in}} = 2n_{\pm} a_3[\text{HOM}]^{(a_4+a_5)/[\text{HOM}]} \quad (7)$$

where the HOMs concentration is given in units of 10^7 molecules per cubic centimetre, n_{\pm} the ion concentration, and a_1 – a_5 are parameters fitted to the experimental data. To account for the fact that the yield of HOMs from endocyclic monoterpenes, such as α -pinene, is higher than that from exocyclic monoterpenes, we separate these classes in our model and use the yields from β -pinene in (Jokinen et al., 2015) to produce HOMs from exocyclic monoterpenes.

We also updated the nanoparticle growth rates (GR) due to organic compounds based on the new measurements from the CLOUD chamber (Tröstl et al., 2016)

$$\text{GR} = 7.3 \times 10^{-8} [\text{H}_2\text{SO}_4] + 1.41 \times 10^{-7} [\text{HOM}].$$

2.1.2. Impact of organic nucleation and growth on global CCN

The new organic-related formation and growth mechanisms described above have been studied individually in several studies (Riccobono et al., 2014; Dunne et al., 2016; Gordon et al., 2016 and Tröstl et al., 2016). In brief, these studies showed that:

- Nucleation of sulphuric acid with oxidation products of α -pinene makes a major contribution to global particle concentrations and helps to explain the seasonal cycle of particle number concentration from biogenic emissions (Riccobono et al., 2014).
- Pure biogenic nucleation of the oxidation products of α -pinene (without sulphuric acid) enhances PI CCN concentrations by 20–100% across large areas of the northern hemisphere and thereby reduces the anthropogenic aerosol-cloud radiative forcing by around 27% (Gordon et al., 2016).
- The treatment of early growth of nucleated particles by condensation of oxidised organic molecules substantially alters global CCN concentrations – by up to $\pm 50\%$ in comparison with previously assumed growth rate parameterizations (Tröstl et al., 2016).
- Organic nucleation is a major factor in global aerosol formation alongside our most complete treatment of inorganic nucleation of sulphuric acid, ammonia and water (Dunne et al., 2016). We estimated that organic nucleation contributes between 28 and 45% of all nucleated particles in the atmosphere.

Within BACCHUS we have assessed the net effect of organic nucleation and early growth on global CCN concentrations, separating out the effect of these two processes from the effect of traditional SOA condensation to larger particles.

Figure 11 shows the effect of organics on CCN in the present day (PD) and the preindustrial (PI, 1750). Tables 2 and 3 summarise the effects. The maps in the middle column of Figure 11 show how the nucleation and growth due to HOMs (equations 4–7) affect CCN and the right column shows the total effect of all SOA (nucleation and growth plus condensation of other SOA components on all aerosols).

There is a marked difference in the effect of organics on CCN in the PI and the PD. In the PI, when aerosol concentrations were lower than present, organic nucleation and growth account for up to 70% of CCN at high latitudes and at least 40% across many continental regions. When condensation of other SOA is included, organics contribute as much as 90% of CCN and generally around 70% across many land areas in the northern hemisphere. In the PD the relative contributions of organics to CCN are reduced compared to the PI, but they are still substantial. The peak contribution of organic nucleation and growth is around 50% in some boreal regions of Eurasia and Canada, and it is at least 20% across most of the northern hemisphere.

The contribution of organics to CCN varies seasonally, driven by the biogenic emissions. In the PI northern hemisphere summer about 52% of surface-level CCN are generated through organic nucleation and growth, but only 23% in winter. The variation is much less in the southern hemisphere (14–17%) due to the much weaker influence of biogenic emissions in controlling CCN over predominantly ocean regions.

The global annual mean summary numbers from Tables 2 and 3 are as follows: Organic nucleation and growth account for 29% of CCN in the PI and 15% in the PD. The total effect of SOA is a 40% contribution to CCN in the PI and 24% contribution in the PD. From these numbers it is clear that organic nucleation and growth is a major factor in CCN production and is also a major component of the overall effect of SOA on CCN: i.e., about three-quarters of the effect of organics on CCN in the PI comes through nucleation and growth and slightly less than two-thirds in the PD.

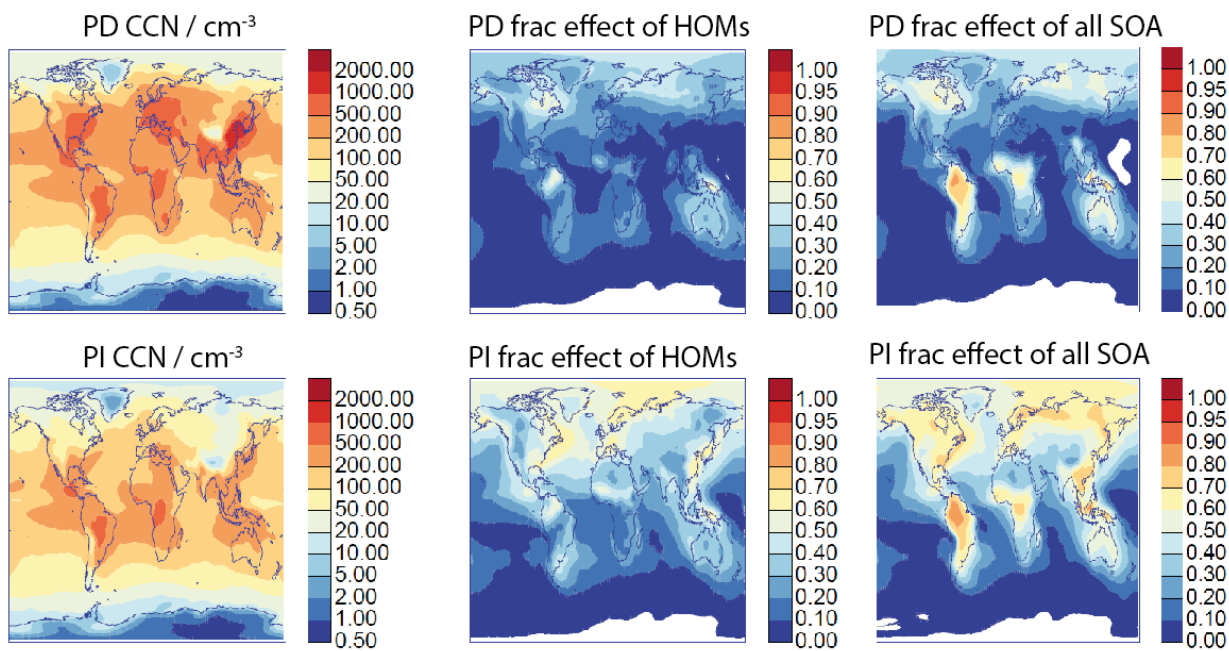


Figure 11. Modelled effect of secondary organic aerosol (SOA) on annual mean CCN concentrations at 0.2% supersaturation in the boundary layer. The left maps show absolute concentrations in the present day (PD) and preindustrial (PI). The middle maps show the fractional contribution to CCN of nucleation and growth caused by highly oxidized organic molecules (HOMs). The right maps show the fractional contribution to CCN of all secondary organic compounds (including nucleation and growth from HOMs as well as SOA condensing on all particles).

Table 2. The percentage contribution to CCN of nucleation and growth caused by highly oxidized organic molecules (HOMs). The results are given as $100 \times (1 - \text{CCN without organic nucleation and growth} / \text{CCN with all processes})$. CCN are reported at several supersaturations and CN refers to all particles larger than 3 nm diameter.

		Jan. NH	Jul. NH	Jan. SH	Jul. SH	Global annual
PD	Surface CN	10.5	57.4	31.6	33.1	37.0
	Surface CCN 0.2%	3.6	31.3	14.4	9.2	15.2
	Cloud base CN	5.4	60.3	38.8	30.0	31.0
	Cloud base CCN 1%	3.8	49.8	28.7	18.1	23.0
	Cloud base CCN 0.2%	3.4	37.1	20.5	11.7	16.4
	High altitude CN	-3.7	8.4	1.1	0.4	-1.6
PI	Surface CN	57.5	83.7	33.6	39.8	62.9
	Surface CCN 0.2%	23.1	51.9	16.8	13.6	28.9
	Cloud base CN	55.2	83.3	43.6	36.4	57.0
	Cloud base CCN 1%	34.2	76.1	34.5	25.6	45.2
	Cloud base CCN 0.2%	25.0	55.8	26.1	16.2	30.1
	High altitude CN	3.7	36.3	5.8	-0.7	4.5

Table 3. The percentage contribution to CCN of all SOA (including HOM contributions to nucleation and growth). The results are given as $100 \times (1 - \text{CCN without SOA} / \text{CCN with all processes})$. CCN are reported at several supersaturations and CN refers to all particles larger than 3 nm diameter.

		Jan. NH	Jul. NH	Jan. SH	Jul. SH	Global annual
PD	Surface CN	8.9	56.2	31.4	32.4	35.7
	Surface CCN 0.2%	13.4	38.0	17.2	21.4	24.4
	Cloud base CN	2.6	58.3	37.6	28.7	28.8
	Cloud base CCN 1%	9.3	54.1	32.6	32.6	29.5
	Cloud base CCN 0.2%	9.4	42.2	24.9	27.4	23.6
	High altitude CN	-6.6	4.0	-2.6	-3.2	-6.1
PI	Surface CN	57.0	82.1	33.6	38.9	61.4
	Surface CCN 0.2%	38.9	58.6	18.1	25.1	39.4
	Cloud base CN	53.9	81.0	42.6	34.8	54.7
	Cloud base CCN 1%	43.7	79.7	36.7	39.4	52.1
	Cloud base CCN 0.2%	36.6	62.5	28.7	32.5	39.2
	High altitude CN	1.7	32.0	4.7	-4.0	0.9

2.1.3. Assessment of model uncertainties

There are many sources of uncertainty that affect these results, and these have been fairly comprehensively assessed in the separate published papers. The uncertainty in parameterized nucleation rates includes components from the CLOUD chamber measurements (measured rates, gas concentrations, and biases in the fit of the parameterization to the data). There are also uncertainties in modelled quantities related to the concentrations of secondary organic molecules produced from terpenes (terpene emissions and yields, growth rates of freshly nucleated aerosol, and the temperature dependence of the organic nucleation rates which was not measured in CLOUD yet).

The uncertainties in the measured nucleation rates are associated with the characterization of the particle counters, especially at low temperatures, and the extrapolation of the measured particle formation rate at 3.2 nm down to the 1.7 nm diameter, which is then implemented in the global model. The overall uncertainty in the modeled nucleation rate at 1.7 nm was estimated to be a factor of 2.5 (Dunne et al., 2016). The effect of increasing modeled inorganic nucleation rates by this factor is about a 2% change in the global PD concentration of 70 nm particles at cloud base level for March-June.

The uncertainties in the organic parameterization (Riccobono et al., 2014) are larger than for the inorganic rates. In particular, the use of a proxy, pinanediol, for monoterpenes introduces an uncertainty in how well the proxy represents the monoterpenes when the results are used in our aerosol model. To attempt to quantify the uncertainties associated with the organic nucleation rates in general terms, we test the effect of using the empirical organic nucleation derived by Paasonen et al. (2010) from field observation data in place of the CLOUD chamber data. They obtained best agreement with particle number observations using

$$J = K_{SA1}[H_2SO_4]^2 + K_{SA2}[H_2SO_4][org], \quad (8)$$

where [org] is the concentration of vapors required to explain the observed growth rates from 2 to 4 nm. In GLOMAP where this process is represented by the oxidation products of terpenes with ozone and with hydroxyl and nitrate radicals. When we introduce the second term in Equation 8 in place of Riccobono et al (equation 4) the global mean change in the concentrations of particles larger than 70 nm in diameter in the PD is only 1.2%. This is less than half of the change in 70 nm particle concentrations due to a possible temperature dependence of the organic nucleation rate (2.8%, see Table 4). Dunne et al. (2016) showed that the global mean fraction of all particles formed via organic nucleation decreases from 31% to 19% with this change of organic nucleation.

The uncertainty in modeled biogenic terpene emissions has been studied by perturbing terpene concentrations by -50% to +100%. This leads to a change of +0.6% in global 70 nm particle concentrations at cloud base level in the PD over March-June.

The lack of experimental data on the temperature dependence of ternary organic nucleation introduces additional uncertainty on the overall fractions of organic and inorganic nucleation in the atmosphere. Introducing a plausible temperature dependence based on quantum chemistry simulations (Dunne et al., 2016) leads to an overall increase in the fraction of organic nucleation below 15 km altitude from 31% to 77% in the PD. This large effect results from an increase in organic nucleation at high altitude. By introducing a temperature dependence relative to the 5°C CLOUD measurements, we found that low altitude nucleation was reduced (where it is warmer than the chamber measurements) but upper troposphere nucleation was increased. Annually averaged, a reduction in 70 nm particle concentrations at cloud base level of 3.6% in the Northern Hemisphere and of 0.8% in the Southern Hemisphere was predicted (Dunne et al., 2016).

Table 4 summarises the sensitivity simulations performed in Dunne et al. (2016) related to organic nucleation effects on CCN in the PD. The largest sources of uncertainty are the terpene emissions (which affect nucleation and growth of all particles). Halving these emissions leads to a 16.6% decrease in CCN (represented in these simulations by particles larger than 70 nm dry diameter). The next most important factor is sulphuric acid concentrations in the model, which could cause at least an 8.5% uncertainty in CCN. Because sulphuric acid is involved in organic nucleation (equation 4), uncertainty in this quantity also has a bearing on our estimates of 'organic-driven' nucleation. The magnitude of the organic nucleation rate,

its temperature dependence and the uncertain organic-driven growth rate are rather unimportant uncertainties in global CCN.

Gordon et al. (2016) presents an analysis of uncertainties related to how pure biogenic nucleation affects PI CCN (equations 5–7). The yield of HOMs from terpene oxidation is the main uncertainty. In the baseline simulations we predicted a 12% increase in PI CCN caused by pure biogenic nucleation. This increased to 19% when the HOMs yield was trebled and fell to 4% when it was reduced to one-third. Including a temperature dependence on the pure biogenic nucleation rate (not measured by CLOUD) reduced the 12% to 7%. These quite large variations are comparable to the effects of other model uncertainties unrelated to organics. For example, a scenario with high primary emissions (see Gordon et al., section S6 for details) reduced the 12% to 7% because the additional aerosol scavenges vapours and nuclei.

Table 4. Summary of sensitivity experiments reported in Dunne et al. (2016) related to organic nucleation in the present-day atmosphere.

Model perturbation	Quantity varied	Change in global mean N70 (%)
Relative humidity	RH dependence of inorganic nucleation	8%
Relative humidity	RH dependence of organic nucleation	Negligible
Organic nucleation rate	Replace Eq. 4 with Eq. 8	-1.2
Model H ₂ SO ₄ (g)	-50/+100%	-8.5/+8.5
T dependence of organic nucleation	Rate in Eq. 4	-2.8
Terpene emissions	-50/+100%	-16.6/+0.6
Nuclei growth rates	-50/+50%	-1.2/+0.6

2.2. ECHAM-HAM and NorESM1 models

Jokinen et al. (2015) implemented the aerosol growth mechanisms due to ELVOC formation to ECHAM-HAM global climate model, and Arneth et al. (2016) further applied this model to the Siberian region. Makkonen et al. (2014) applied SOA formation, organic nucleation and subsequent growth in NorESM1. In Jokinen et al. (2015), SOA was assumed to form via three precursors: endocyclic monoterpenes, other monoterpenes, and isoprene. All three precursors were linked to the formation of ELVOCs and SVOCs after oxidation by OH, O₃ and NO₃. ELVOCs were allowed to participate in nucleation and early growth of sub-10 nm particles.

The analysis in Jokinen et al. (2015) indicated a globally important 1) contribution to the particle growth from ELVOCs, and 2) reduction in NPF due to increased sink from SVOCs formation from isoprene. Figure 12 shows organic aerosol size distribution with and without SOA formation. ELVOCs increase CN concentrations, and this increase is even several tens of % regionally. While the effect on CCN at 1.0%

supersaturation from the increased aerosol growth due to ELVOCs was relatively large, the contribution to larger sizes (CCN at 0.2% supersaturation) remains modest in modal M7 framework (Jokinen et al., 2015). M7 describes the aerosol population using 7 log-normal modes: a nucleation mode and two modes in the Aitken, accumulation and coarse particle size ranges. While SVOCs from isoprene increase CCN concentrations at 0.2% supersaturation, the increased sinks results in decreased CN concentrations.

Arneth et al. (2016) applied the ELVOC formation mechanisms to Siberian domain, and found that projected future increase of BVOC emission in the region provides a means for increased nucleation and aerosol growth rates, leading to increased CCN concentrations (Figure 13).

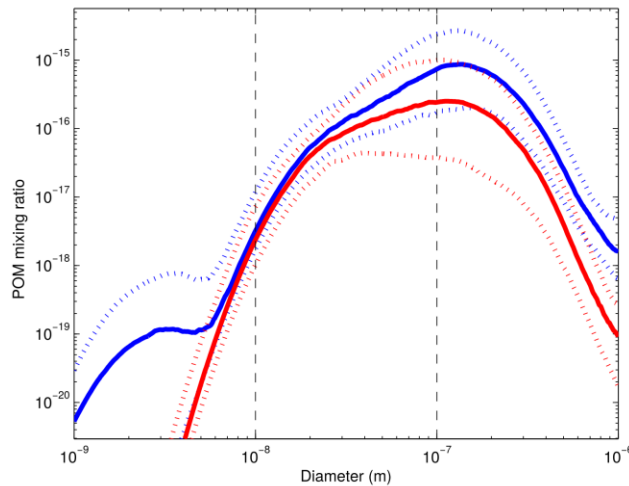


Figure 12. Annual average particulate organic matter mixing ratio in Hyytiälä, as simulated by ECHAM-HAM. The blue line indicates simulation with ELVOC+SVOC formation (Jokinen et al., 2015), while red line shows simulation without SOA formation. ELVOC formation allows organics to participate in nucleation and early growth, hence SOA simulation (blue) shows significant increase in sub-10nm organic concentration. Major portion of total SOA is formed in accumulation mode particle size

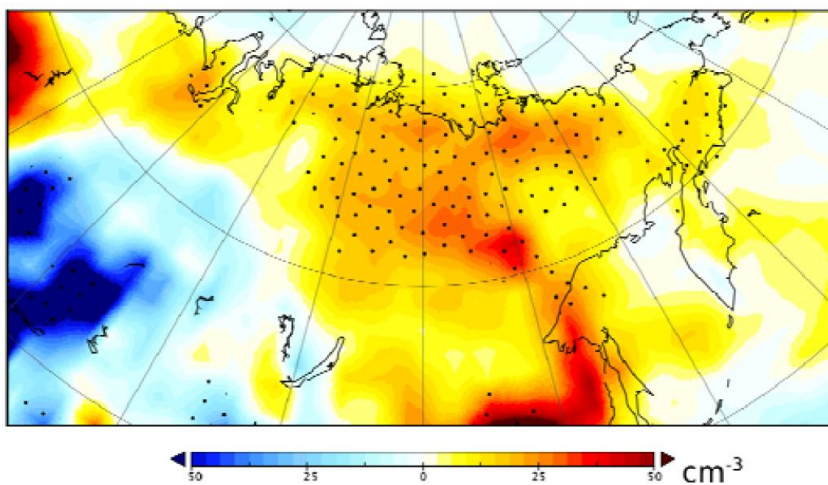


Figure 13. Annual average increase in Siberian CCN(1.0%) due to increase in BVOC emissions between 2000 and 2100. (From Arneth et al. 2016).

3. Reference list

Arneth, A., Makkonen, R., Olin, S., Paasonen, P., Holst, T., Kajos, M. K., Kulmala, M., Maximov, T., Miller, P. A., and Schurgers, G.: Future vegetation–climate interactions in Eastern Siberia: an assessment of the competing effects of CO₂ and secondary organic aerosols, *Atmos. Chem. Phys.*, 16, 5243-5262, 2016.

Charlson, R. J., Lovelock, J. E., Andreae, M. O., and Warren, S. G.: Oceanic Phytoplankton, Atmospheric Sulfur, Cloud Albedo and Climate, *Nature*, 326, 655-661, 1987.

Dall'Osto, M., Ceburnis, D., Monahan, C., Worsnop, D. R., Bialek, J., Kulmala, M., Kurten, T., Ehn, M., Wenger, J., Sodeau, J., Healy, R., and O'Dowd, C.: Nitrogenated and aliphatic organic vapors as possible drivers for marine secondary organic aerosol growth, *J. Geophys. Res.*, 117, 10.1029/2012jd017522, 2012.

Donahue N. M., Epstein S. A., Pandis S. N. and Robinson A. L.: A two dimensional volatility basis set: 1. organic-aerosol mixing thermodynamics, *Atmos. Chem. Phys.*, 11, 3303–3318, 2011.

Dunne, E. M. et al.: Global atmospheric particle formation from CERN CLOUD experiments. *Science*, DOI: 10.1126/science.aaf2649, 2016.

Ehn M., Thornton J. A., Kleist E., Sipilä M., Junninen H., Pullinen I., Springer M., Rubach F., Tillmann R., Lee B., Lopez-Hifiker F., Andres S., Acir I.H., Rissanen M., Jokinen T., Schobesberger S., Kangasluoma J., Kontkanen J., Nieminen T., Kurten T., Nielsen L. B., Jorgensen S., Jaergaard H. G., Canagaratna M., Dal Maso M., Berndt T., Petäjä T., Wahner A., Kerminen V.-M., Kulmala M., Worsnop D., Wildt J. and Mentel T. F.: A large source of low-volatility secondary organic aerosol, *Nature*, 506, 476-479, 2016.

Facchini, M. C., Decesari, S., Rinaldi, M., Carbone, C., Finessi, E., Mircea, M., Fuzzi, S., Moretti, F., Tagliavini, E., Ceburnis, D., and O'Dowd, C. D.: Important source of marine secondary organic aerosol from biogenic amines, *Environ. Sci. Technol.*, 42, 9116-9121, doi:10.1021/Es8018385, 2008.

Gordon, H., Sengupta, K., Rap, A., Duplissy, J., Frege, C., Williamson, C., Heinritzi, M., Simon, M., Yan, C., Almeida, J., Trostl, J., Nieminen, T., Ortega, I. K., Wagner, R., Dunne, E. M., Adamov, A., Amorim, A., Bernhammer, A.-K., Bianchi, F., Breitenlechner, M., Brilke, S., Chen, X., Craven, J. S., Dias, A., Ehrhart, S., Fischer, L., Flagan, R. C., Franchin, A., Fuchs, C., Guida, R., Hakala, J., Hoyle, C. R., Jokinen, T., Junninen, H., Kangasluoma, J., Kim, J., Kirkby, J., Krapf, M., Kuerten, A., Laaksonen, A., Lehtipalo, K., Makhmutov, V., Mathot, S., Molteni, U., Monks, S. A., Onnela, A., Perakyla, O., Piel, F., Petaja, T., Praplan, A. P., Pringle, K. J., Richards, N. A. D., Rissanen, M. P., Rondo, L., Sarnela, N., Schobesberger, S., Scott, C E., Seinfeld, J. H., Sharma, S., Sipilä, M., Steiner, G., Stozhkov, Y., Stratmann, F., Tome, A., Virtanen, A., Vogel, A. L., Wagner, A. C., Wagner, P. E., Weingartner, E., Wimmer, D., Winkler, P. M., Ye, P., Zhang, X., Hansel, A., Dommen, J., Donahue, N. M., Worsnop, D. R., Baltensperger, U., Kulmala, M., Curtius, J., Carslaw, K. S.: Reduced anthropogenic aerosol radiative forcing caused by biogenic new particle formation, *Proc. Natl. Acad. Sci. USA*, 43, 12053-12058, 2016.

Jokinen T., Berndt, T., Makkonen R., Kerminen V.-M., Junninen H., Paasonen P., Stratmann F., Herrmann H., Guenther A., Worsnop D. R., Kulmala M., Ehn M. and Sipilä M.: Production of extremely low-volatile organic compounds from biogenic emissions: measured yields and atmospheric implications. *Proc. Nat. Acad. Sci.*, 112, 7123-7128, 2015.

Kalivitis N., Kerminen V.-M., Kouvarakis G., Stavroulas I., Bougiatioti A., Nenes A., Manninen H. E., Petäjä T., Kulmala M. and Mihalopoulos N.: Atmospheric new particle formation as a source of CCN in the eastern Mediterranean marine boundary layer, *Atmos. Chem. Phys.*, **15**, 9203-9215, 2015.

Kazil, J., Stier, P., Zhang, K., Quaas, J., Kinne, S., O'Donnell, D., Rast, S., Esch, M., Ferrachat, S., Lohmann, U., and Feichter, J.: Aerosol nucleation and its role for clouds and Earth's radiative forcing in the aerosol-climate model ECHAM5-HAM, *Atmos. Chem. Phys.*, **10**, 10733–10752, 2010.

Kerminen V.-M., Paramonov M., Anttila T., Riipinen I., Fountoukis C., Korhonen H., Asmi, E., Laakso L., Lihavainen H., Swietlicki E., Svenningsson B., Asmi A., Pandis S. N., Kulmala M. and Petäjä T.: Cloud condensation nuclei production associated with atmospheric nucleation: a synthesis based on existing literature and new results, *Atmos. Chem. Phys.*, **12**, 12037-12059, 2012.

Kirkby J., Duplissy J., Sengupta K., Frege C., Gordon H., Williamson C., Heinritzi M., Simon M., Yan C., Almeida J., Tröstl J., Nieminen T., Ortega I. K., Wagner W., Adamov A., Amorim A., Bernhammer A.-K., Bianchi F., Breitenlechner M., Brilke S., Chen X., Craven J., Dias A., Ehrhart S., Flagan R. C., Franchin A., Fuchs C., Guida R., Hakala J., Hoyle C. R., Jokinen T., Junninen H., Kangasluoma J., Kim J., Krapf M., Kürten A., Laaksonen A., Lehtipalo K., Makhmutov V., Mathot S., Molteni U., Onnela A., Peräkylä O., Piel F., Petäjä T., Praplan A. P., Pringle K., Rap A., Richards N. A. D., Riipinen I., Rissanen M. P., Rondo L., Sarnela N., Schobesberger S., Scott C. E., Seinfeld J. H., Sipilä M., Steiner G., Stozhkov Y., Stratmann F., Tomé A., Virtanen A., Vogel A. L., Wagner A. C., Wagner P. E., Weingartner E., Wimmer D., Winkler P., Ye P., Zhang X., Hansel A., Dommen J., Donahue N. M., Worsnop D. R., Baltensperger U., Kulmala M., Carslaw K. S. and Curtius J.: Ion-induced nucleation of pure biogenic particles, *Nature*, **533**, 521–526, 2016.

Kontkanen J., Paasonen P., Aalto J., Bäck J., Rantala P., Petäjä T. and Kulmala M.: Simple proxies for estimating the concentrations of monoterpenes and their oxidation products at a boreal forest site, *Atmos. Chem. Phys.*, **16**, 13291-13307, 2016.

Kulmala M., Petäjä T., Ehn M., Thornton J., Sipilä M., Worsnop D. R. and Kerminen V.-M.: Chemistry of atmospheric nucleation: On the recent advances on precursor characterization and atmospheric cluster composition in connection with atmospheric new particle formation, *Annu. Rev. Phys. Chem.*, **65**, 21-37, 2014.

Lehtipalo K., Rondo L., Kontkanen J., Schobesberger S., Jokinen T., Sarnela N., Kürten A., Ehrhart S., Franchin A., Nieminen T., Riccobono F., Sipilä M., Yli-Juuti T., Duplissy J., Adamov A., Ahlm L., Almeida J., Amorim A., Bianchi F., Breitenlechner M., Dommen J., Downard A., Dunne E., Flagan R., Guida R., Hakala J., Hansel A., Jud W., Kangasluoma J., Kerminen V.-M., Keskinen H., Kim J., Kirkby J., Kupc A., Kupiainen-Määttä O., Laaksonen A., Lawler M., Leiminger M., Mathot S., Olenius T., Ortega I., Onnela A., Petäjä T., Praplan A., Rissanen M., Ruuskanen T., Santos F., Schallhart S., Schnitzhofer R., Simon M., Smith J., Troestl J., Tsagkogeorgas G., Tome A., Vaattovaara P., Vehkamäki H., Virtala A., Wagner P., Williamson C., Wimmer D., Winkler P., Virtanen A., Donahue N., Carslaw K., Baltensperger U., Riipinen I., Curtius J., Worsnop D. and Kulmala M.: The effect of acid-base clustering and ions on the growth of atmospheric nanoparticles, *Nature Communications*, **7**, 11594, doi:10.1038/ncomms11594, 2016.

Makkonen, R., Seland, Ø., Kirkevåg, A., Iversen, T., and Kristjánsson, J. E.: Evaluation of aerosol number concentrations in NorESM with improved nucleation parameterization, *Atmos. Chem. Phys.*, **14**, 5127-5152, 2014.

Makkonen, R., Seland, Ø., Kirkevåg, A., Iversen, T., and Kristjánsson, J. E.: Evaluation of aerosol number concentrations in NorESM with improved nucleation parameterization, *Atmos. Chem. Phys.*, **14**, 5127-5152, doi:10.5194/acp-14-5127-2014, 2014.

Merikanto, J., Spracklen, D. V., Pringle, K. J., and Carslaw, K. S.: Effects of boundary layer particle formation on cloud droplet number and changes in cloud albedo from 1850 to 2000, *Atmos. Chem. Phys.*, **10**, 695–705, 2010.

O'Dowd, C., Monahan, C., and Dall'Osto, M.: On the occurrence of open ocean particle production and growth events, *Geophys. Res. Lett.*, **37**, L19805, 10.1029/2010GL044679, 2010.

Paasonen P., Nieminen T., Asmi E., Manninen H. E., Petäjä T., Plass-Dülmer C., Flentje H., Birmili W., Wiedensohler A., Horrak U., Metzger A., Hamed A., Laaksonen A., Facchini M. C., Kerminen V.-M. and Kulmala M.: On the roles of sulphuric acid and low-volatility organic vapours in the initial steps of atmospheric new particle formation, *Atmos. Chem. Phys.*, **10**, 11223-11242, 2010.

Pierce, J. R. and Adams, P. J.: Uncertainty in global CCN concentrations from uncertain aerosol nucleation and primary emission rates, *Atmos. Chem. Phys.*, **9**, 2009.

Qi X. M., Ding A. J., Nie W., Petäjä T., Kerminen V.-M., Herrmann E., Xie Y. N., Zheng L. F., Manninen H., Aalto P., Sun J. N., Xu Z. N., Chi X. G., Huang X., Boy M., Virkkula A., Yang X.-Q., Fu. C. B. and Kulmala M.: Aerosol size distribution and new particle formation in the western Yangtze River Delta of China: 2 years of measurements at the SORPES station, *Atmos. Chem. Phys.*, **15**, 12445-12464, 2015.

Riccobono F., Schobesberger S., Scott C. E., Dommen J., Ortega I. K., Rondo L., Almeida J., Amorim A., Bianchi F., Breitenlechner M., David A., Downard A., Dunne E.M., Duplissy J., Ehrhart S., Flagan R. C., Franchin A., Hansel A., Junninen H., Kajos M., Keskinen H., Kupc A., Kürten A., Kvashin A. N., Laaksonen A., Lehtipalo K., Makhmutov V., Mathot S., Nieminen T., Onnela A., Petäjä T., Praplan A.P., Santos F.D., Schallhart S., Seinfeld J. H., Sipilä M., Spracklen D. V., Stozhkov Y., Stratmann F., Tomé A., Tsagkogeorgas G., Vaattovaara P., Viisanen Y., Vrtala A., Wagner P.E., Weingartner E., Wex H., Wimmer D., Carslaw K. S., Curtius J., Donahue N. M., Kirkby J., Kulmala M., Worsnop D. R. and Baltensperger U.: Oxidation Products of Biogenic Emissions Contribute to Nucleation of Atmospheric Particles, *Science*, **344**, 717-721, 2014.

Sipilä M., Sarnela N., Jokinen T., Henschel H., Junninen H., Kontkanen J., Richters S., Kangasluoma J., Franchin A., Peräkylä O., Rissanen M. P., Ehn M., Vehkamäki H., Kurten T., Berndt T., Petäjä T., Worsnop D., Ceburnis D., Kerminen V.-M., Kulmala M. and O'Dowd C. D.: Molecular-scale evidence of aerosol particle formation via sequential addition of HIO₃, *Nature*, **537**, 532-534, doi:10.1038/nature19314, 2016.

Tröstl J., Chuang W. K., Gordon H., Heinritzi G., Yan C., Molteni U., Ahlm L., Frege C., Bianchi F., Wagner R., Simon M., Lehtipalo K., Williamson C., Craven J. S., Duplissy J., Adamov A., Almeida J., Bernhammer A.-K., Breitenlechner M., Brilke S., Dias A., Ehrhart S., Flagan R. C., Franchin A., Fuchs C., Guida R., Gysel M., Hansel A., Hoyle R. C., Jokinen T., Junninen H., Kangasluoma J., Keskinen H., Kim J., Krapf M., Kürten A., Laaksonen A., Lawler M., Leiminger M., Mathot S., Möhle O., Nieminen T., Onnela A., Petäjä T., Piel F. M., Miettinen S., Rissanen M. P., Rondo L., Sarnela N., Schobesberger S., Sengupta K., Sipilä M., Smith J. N., Steiner G., Tomes A., Virtanen A., Wagner A. C., Weingartner E., Wimmer D., Winkler P. M., Ye P., Carslaw K. S., Curtius J., Dommen J., Kirkby J., Kulmala M., Riipinen I., Worsnop D. R., Donahue N. M. and Baltensperger U.: The role of low-volatility organic compounds in initial particle growth in the atmosphere, *Nature*, **533**, 527-531, 2016.

Vaishya, A., Ovadnevaite, J., Bialek, J., Jennings, S. G., Ceburnis, D., and O'Dowd, C. D.: Bistable effect of organic enrichment on sea spray radiative properties, *Geophys. Res. Lett.*, 40, 6395-6398, 10.1002/2013gl058452, 2013.

Changes with respect to the DoW

No changes with respect to DoW

Dissemination and uptake

The parameterizations are available for the BACCHUS modeling groups to be implemented in regional and global models.

BACCHUS has contributed to the following peer-reviewed publications:

Arneth, A., Makkonen, R., Olin, S., Paasonen, P., Holst, T., Kajos, M. K., Kulmala, M., Maximov, T., Miller, P. A., and Schurgers, G.: Future vegetation–climate interactions in Eastern Siberia: an assessment of the competing effects of CO₂ and secondary organic aerosols, *Atmos. Chem. Phys.*, 16, 5243-5262, doi:10.5194/acp-16-5243-2016, 2016.

Kalivitis N., Kerminen V.-M., Kouvarakis G., Stavroulas I., Bougiatioti A., Nenes A., Manninen H. E., Petäjä T., Kulmala M. and Mihalopoulos N.: Atmospheric new particle formation as a source of CCN in the eastern Mediterranean marine boundary layer, *Atmos. Chem. Phys.*, 15, 9203-9215, 2015.

Makkonen, R., Seland, Ø., Kirkevåg, A., Iversen, T., and Kristjánsson, J. E.: Evaluation of aerosol number concentrations in NorESM with improved nucleation parameterization, *Atmos. Chem. Phys.*, 14, 5127-5152, doi:10.5194/acp-14-5127-2014, 2014.

Jokinen, T., Berndt, T., Makkonen, R., Kerminen, V.-M., Junninen, H., Paasonen, P., Stratmann, F., Herrmann, H., Guenther, A.B., Worsnop, D.R., Kulmala, M., Ehn, M. and Sipilä, M.: Production of extremely low volatile organic compounds from biogenic emissions: Measured yields and atmospheric implications, *PNAS*, 112 (23), 7123-7128, 2015.

Tröstl J., Chuang W. K., Gordon H., Heinritzi G., Yan C., Molteni U., Ahlm L., Frege C., Bianchi F., Wagner R., Simon M., Lehtipalo K., Williamson C., Craven J. S., Duplissy J., Adamov A., Almeida J., Bernhammer A.-K., Breitenlechner M., Brilke S., Dias A., Ehrhart S., Flagan R. C., Franchin A., Fuchs C., Guida R., Gysel M., Hansel A., Hoyle R. C., Jokinen T., Junninen H., Kangasluoma J., Keskinen H., Kim J., Krapf M., Kürten A., Laaksonen A., Lawler M., Leiminger M., Mathot S., Möhle O., Nieminen T., Onnela A., Petäjä T., Piel F. M., Miettinen S., Rissanen M. P., Rondo L., Sarnela N., Schobesberger S., Sengupta K., Sipilä M., Smith J. N., Steiner G., Tomes A., Virtanen A., Wagner A. C., Weingartner E., Wimmer D., Winkler P. M., Ye P., Carslaw K. S., Curtius J., Dommen J., Kirkby J., Kulmala M., Riipinen I., Worsnop D. R., Donahue N. M. and Baltensperger U.: The role of low-volatility organic compounds in initial particle growth in the atmosphere, *Nature*, 533, 527-531, 2016.